Conformations and Rotational Barriers of Aromatic Polyesters. 3. AM1-Based Parametrization of a Force Field for Poly(*p*-hydroxybenzoic acid) and for Poly(6-hydroxy-2-naphthoic acid)

Jippe van Ruiten and Robert J. Meier*

DSM Research, P.O. Box 18, 6160 MD Geleen, The Netherlands

Christoph Hahn, Thomas Mosell, Alla Sariban, and Jürgen Brickmann

Institut für Physikalische Chemie I, Technische Hochschule Darmstadt, Petersenstrasse 20, DW-6100 Darmstadt, Federal Republic of Germany

Received June 23, 1992; Revised Manuscript Received November 13, 1992

ABSTRACT: Force fields with good transferrability for poly(*p*-hydroxybenzoic acid) and for poly(6-hydroxy-2-naphthoic acid) were developed on the basis of a fit of the force field parameters to the results from semiempirical AM1 calculations. The dihedral terms in the force field describing the rotations in the ester linkages are the most important ingredients with respect to modeling of the conformational properties of these macromolecules. These torsional barriers were scaled by a factor of 1.9 as proposed in the second paper of this series. Very good agreement between the scaled AM1 potential energy surface and the fitted force field was obtained. When employing such a proper force field, molecular dynamics simulations do show substantial differences in flexibility with respect to bond rotation in single isolated chains as compared to the use of a "standard" force field.

1. Introduction

In the first paper of this series,[1a] we have extensively discussed the difficulties encountered when modeling the conformational properties of aromatic polyesters at the molecular level (ref 1b is a Comment by Jung and Schürmann; ref 1c is our Response to that Comment). It was demonstrated in that paper that different theoretical methods yielded quite different values for the rotational barrier heights, the latter being an essential ingredient with respect to the modeling of polymer chain conformations. No method could a priori be said to be the most reliable one. It was also noted that this is a topic hardly considered in other published papers. Another problem is the inclusion of bulk effects into the parametrization of force fields. The use of data obtained from crystal structures and measurements in solution makes it possible to replace purely energetic force field terms by a potential of mean force that shall account for the effects of the environment. As a result, simulations of a single chain can be performed to obtain results valid for the bulk state. The large amount of computer time necessary to perform simulations of macromolecules makes this single-chain approach the most feasible approach to the simulation of macromolecules. However, this approach makes it impossible to assign any results on chain flexibility to properties inherent to the molecular structure of the chain, as a preference of linear chain structures may have been imposed by crystalline (or main-chain liquid crystalline) structures, while the chains themselves would be much more flexible when no environment effects are taken into account. The exact effects of the environment at the molecular level are unknown. The potential of mean force should depend on the local molecular structure, and therefore chemical substitution should strongly influence this quantity. These changes cannot be taken into consideration if a (force field) parametrization includes the environment on such a basis. The crucial point here is that the force field parameters are a mixture of the inter- and intramolecular interactions in a way that they cannot be separated afterward. We envision developing a force field in which intra- and intermolecular interactions are well separated, and which, as we hope, can finally be used for molecular design of structures.

Then in the second part of this series[2] it was shown from data on benzaldehyde, for which an accurate gas-phase rotational barrier value is available, that treatment at the ab initio level requires very extensive ab-initio calculations including electron-correlation treatment at the MCSCF level to obtain good agreement with experiment. Their computational expense makes such extensive calculations impractical when they have to be carried out on a series of such aromatic moieties, and they are unfeasible for polymeric structures. It was subsequently shown[2] by comparing experimental gas-phase data on small aromatic moieties having a conjugated substituent with results from semiempirical calculations employing the AM1 method[3] that a single scaling factor can be introduced that relates the experimental gas phase to the AM1 calculated rotational barrier heights. This involves multiplying the AM1 calculated rotational energies of these aromatic fragments by 1.9, which then yielded the experimental gas-phase barrier within 15% accuracy, a thus far unequalled success.

Although it is evident that this is a pragmatic approach, it is both feasible and more accurate than any other theoretical method employed so far and, consequently, of practical importance with respect to polymer modeling. Now that this approach has been proved to be useful, it becomes a matter of implementing it. This is the subject of the present paper. Equilibrium structures as predicted by the AM1 method are generally speaking sufficiently reliable[3–5] for the purpose of polymer modeling. Since the modeling of large molecular structures such as polymers is only feasible when using force field (FF) methods, we have employed the AM1 calculated potential energy surface with proper scaling (aforementioned factor of 1.9) of the rotational barrier heights as the basis to which we have fitted a force field expression. Staying with the same type of molecules as in part 1, we have fitted force fields for dimers of *p*-hydroxybenzoic acid and 6-hydroxy-2-

0024-9297/93/2226-1555$04.00/0

naphthoic acid (for structures see Figure 1), which for convenience we will refer to by their abbreviated polymer names PHBA and PHNA, respectively. One might now object that such force fields refer to the gas phase only for the parameter fit has been partly carried out by reference to gas-phase data (the torsional barrier scaling). This point will be discussed at the end of section 5.

The rest of this paper consists of the following sections. The next section contains a brief account of the computational procedures used. Then in section 3 the employed force field expression is introduced. The procedure of fitting the FF parameters is discussed in section 4. In section 5 the results of the semiempirical AM1 calculations and the fitted force field results are presented. Before we end up with the main conclusions from this work, in section 6 we discuss the consequences for polymer conformational characteristics as obtained from molecular dynamics simulations on PHBA employing the newly derived force fields for these species.

2. Computational Methods

Semiempirical AM1[3] calculations were carried out on an IBM-3090-VF with the AM1 version contained in the MOPAC5.0 suite of programs.[6] The AM1 calculated torsional energy surfaces were fitted to a given force field expression (explicit form to be discussed in the next section). For that purpose a special computer program was developed on the basis of the NAG routine E04NCF which enables a linear least-squares fit with linear boundary conditions and the possibility of fixing accessible parameter intervals as additional constraints.

The MD simulations and force field minimizations with the new force field were also carried out on the IBM-3090 using a MD program developed at TH Darmstadt. The reference MD simulations involving one of the "older" force fields were carried out by employing the consistent valence force field (CVFF)[7] and the MD program as incorporated in the INSIGHT/DISCOVER molecular modeling software package[8] running on a Silicon Graphics 4D/25GT workstation. The force field minimizations were carried out with 1.3-fs time steps and by setting the temperature equal to 0.0009 K. The torsional potential was probed by varying the torsional angle stepwise. At every such increase of the torsional angle, the temperature increased somewhat and the system was subsequently cooled to 0.0009 K again to enable the system to find its minimum energy conformation. Fixing of the bond lengths and fixing of the benzene and naphthalene core were realized by employing a combination of the SHAKE algorithm[9] and a method developed by Ciccotti et al.[10]

3. Force Field Expression

The force field to be discussed now was primarily developed to describe the rotational barriers in PHBA and PHNA, although the other force field terms were fully accounted for as well. As model systems for these polymers we have taken the corresponding dimers and trimers. The structures are depicted in Figure 1, where we have also indicated our nomenclature for the torsional angles, i.e. E, F, and G. Since it is intended to employ the force field in molecular dynamics (MD) calculations as well, it is recommended that a minimum number of force field terms be used. Therefore, bond lengths were kept fixed because they have a negligible contribution to the conformational changes. Such an approach allows for larger time steps in the MD simulations. Both the benzene and the naphthalene core were considered rigid, i.e., valence, torsional, and out-of-plane terms were kept fixed.

We have employed the following force field expression:

$$V = \sum_{ijk} V_{\text{valence},ijk} + \sum_{ijkl} V_{\text{torsion},ijkl} + \sum_{ijkl} V_{\text{improper torsion},ijkl} + \sum_{ij} V_{\text{vdW},ij} + \sum_{ij} V_{\text{Coulomb},ij}$$

$$V = \sum_{ijk} {}^1/_2 k_v(\Theta_{ijk} - \Theta_{ijk,0})^2 + \sum_{ijkl}\sum_{n=1}^{4} H_{n\phi}(1 - \cos(n\phi_{ijkl})) + \sum_{ijkl} H_{2\Phi}(1 - \cos(2\Phi_{ijkl})) + \sum_{ij} 4\epsilon_{ij}[(\sigma_{ij}/r_{ij})^{12} - (\sigma_{ij}/r_{ij})^{6}] + \sum_{ij} (4\pi\epsilon_0 r_{ij})^{-1} q_i q_j \quad (1)$$

The distinct atom types present in the PHBA and PHNA species are defined in Table I. The Lennard-Jones (LJ) parameters for interactions between like atoms were taken from the AMBER force field.[11] The LJ parameters for interactions between nonlike atoms were obtained by applying the Lorentz–Berthelot rule[12] $\epsilon_{ij} = (\epsilon_{ii}\epsilon_{jj})^{1/2}$, $\sigma_{ij} = (\sigma_{ii} + \sigma_{jj})/2$. A single change in some of the LJ parameters as incorporated in the AMBER force field was adopted as shown in the last line of Table II. This was necessary because for the structures with $F = 180°$ and $G = 0°, 180°$, the carbonyl oxygen and a phenyl hydrogen are very close and, when using the standard AMBER parameters, their mutual distance implies an interaction in the strongly repulsive part of the Lennard-Jones potential. To amend this deficiency, the relevant LJ parameters (atom pairs 20/28 and 20/30 in PHNA and atom pairs 19/20 and 19/25 in PHBA) were adapted to have the force field optimized minimum energy geometry to be well-fitted to the AM1 minimized geometry. The LJ parameter values actually employed in this study have been collected in Table II.

Charges were adopted from the Mulliken population analysis following AM1 calculations (see Tables III and IV) as revealed from the corresponding minimum energy structures of the dimeric species depicted in Figure 1. Charges were assigned such that atoms that can be rotated into equivalent positions, e.g., hydrogens H_{18} and H_{29} in PHBA (Figure 1), have been assigned identical charges; these charges were obtained by averaging the AM1 calculated charges of the respective atoms. When the partial charge on an atom was found to be significantly dependent on the conformation (i.e., in the present case dependent on the torsional state), a charge was assigned corresponding to the average over all of these conformations. When this scheme is adopted, the charges are kept constant and the torsional potential is practically fully represented by the torsional term $V_{\text{torsion},ijkl}$ in eq 1. Evidently care is taken in this procedure that electroneutrality is conserved.

Because the force field is finally intended to be applied to polymer chains, the electroneutrality condition should still be satisfied in structures larger than the dimers; i.e., the extension of the polymer chain by one monomer unit should not alter the total charge of the molecule. The charge distribution of an additional monomer unit was studied from AM1 calculations on trimers of HBA and HNA. The calculated charges for the extension unit were taken from the central monomer in the trimer. Values have been collected in Tables V and VI for PHNA and PHBA, respectively.

4. Force Field for PHBA and PHNA and Force Field Fit Procedure

Full geometry optimizations were carried out by employing the AM1 method and varying the relevant three torsional angles of the ester groups in model systems

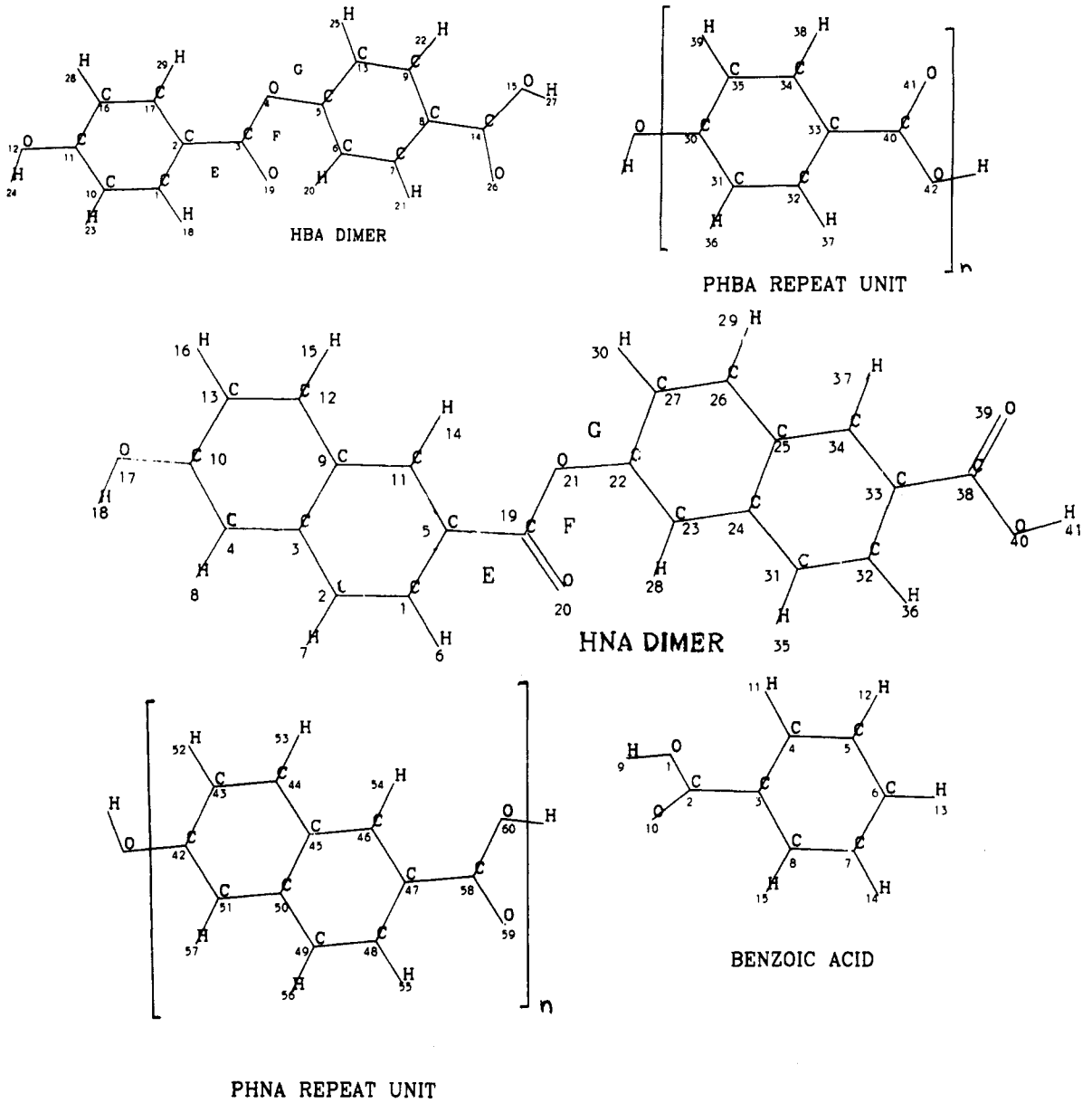

Figure 1. Model systems for *p*-hydroxybenzoic acid and 6-hydroxy-2-naphthoic acid. Depicted are the corresponding dimers, the respective (monomer) repeat units, and benzoic acid.

Table I
Definition of Atom Types in the Force Field Equation 1

atom	description	type
H	hydrogen atoms (bonded to carbon)	10
	protic hydrogen	11
C	carbonyl carbon	63
	aromatic carbon (except for α-position in naphthalene ring)	65
	aromatic carbon: α-position in naphthalene ring	66
O	oxygen in hydroxyl group, including those in a carboxyl group	80
	ether oxygen in an ester group	83
	carbonyl oxygen	85

corresponding to dimers of PHBA and PHNA. Both structures are depicted in Figure 1. The torsional angles were subsequently increased in fixed increments of 15°. While this torsional angle was fixed, all other geometrical variables were (re)optimized. Some problems occurred, in particular for torsion *F* in both PHBA and PHNA. The problem is that while rotating around torsion *F*, the energy minimization procedure, both in the MOPAC program as well as in the MD simulation program when employed as an energy minimizer, does not find the proper saddle point on the potential energy surface. Instead, a local minimum "valley" is followed until a sharp drop in energy arises because suddenly quite a different structure is found with lower energy. This feature is the result of the concerted motion between the dihedrals whose occurrence was reported before.[1a] The sharp drop in energy is due to the fact that, after a local saddle point is reached, a new local minimum energy structure is found by optimization of other coordinates (e.g., torsions *E* and *G*) that are coupled with torsion *F*. To circumvent the problem that the concerted motion prevents from getting to various regions of dihedral space, we have calculated two-dimensional maps of torsions *F* vs *G* with 30° increments, which resulted in a contour map of 13 × 13 energy data points (Figure

Table II
Lennard-Jones Parameters for Like Atom Pairs; for Unlike Atom Pairs the Lorentz–Berthelot Rule Has Been Applied (for Explanation See Text)

atom	type	Lennard-Jones parameter σ (Å)	Lennard-Jones parameter ε (kcal/mol)
H	10	2.74	0.01
	11	1.78	0.02
C	63	3.296	0.12
	65	3.296	0.12
	66	3.296	0.12
O	80	2.94	0.15
	83	2.94	0.15
	85	2.85	0.20
combination of atoms 20/28, 20/30 (PHNA); 19/20, 19/25 (PHBA)		2.20	0.312

Table III
AM1 Calculated Partial Charges for the PHNA Dimer (for Comments See Text)

atom no.	atom	type	charge	atom no.	atom	type	charge
1	C	65	−0.07	22	C	65	+0.10
2	C	66	−0.14	23	C	66	−0.14
3	C	65	+0.02	24	C	65	+0.01
4	C	66	−0.17	25	C	65	−0.08
5	C	65	−0.13	26	C	66	−0.09
6	H	10	+0.15	27	C	65	−0.14
7	H	10	+0.15	28	H	10	+0.15
8	H	10	+0.15	29	H	10	+0.15
9	C	65	−0.09	30	H	10	+0.15
10	C	65	+0.10	31	C	66	−0.13
11	C	66	−0.03	32	C	65	−0.08
12	C	66	−0.07	33	C	65	−0.12
13	C	65	−0.20	34	C	66	−0.03
14	H	10	+0.15	35	H	10	+0.15
15	H	10	+0.15	36	H	10	+0.15
16	H	10	+0.15	37	H	10	+0.15
17	O	80	−0.25	38	C	63	+0.36
18	H	11	+0.22	39	O	85	−0.36
19	C	63	+0.36	40	O	80	−0.32
20	O	85	−0.34	41	H	11	+0.25
21	O	83	−0.24				

Table IV
AM1 Calculated Partial Charges for the PHBA Dimer (for Comments See Text)

atom no.	atom	type	charge	atom no.	atom	type	charge
1	C	65	−0.02	16	C	65	−0.18
2	C	65	−0.16	17	C	65	−0.02
3	C	63	+0.36	18	H	10	+0.15
4	O	83	−0.24	19	O	85	−0.34
5	C	65	+0.13	20	H	10	+0.15
6	C	65	−0.16	21	H	10	+0.15
7	C	65	−0.04	22	H	10	+0.15
8	C	65	−0.14	23	H	10	+0.15
9	C	65	−0.04	24	H	11	+0.18
10	C	65	−0.18	25	H	10	+0.15
11	C	65	+0.12	26	O	85	−0.36
12	O	80	−0.24	27	H	11	+0.25
13	C	65	−0.16	28	H	10	+0.15
14	C	63	+0.36	29	H	10	+0.15
15	O	80	−0.32				

5a). So the reasons for the use of this map are (i) the map contains data points which are closer to the actual saddle point and (ii) the map allows for an additional check whether the torsional force field parameters are suitable for describing a whole series of (*F*,*G*) combinations rather than just the limited set obtained by varying one of the torsional angles and optimizing all other degrees of freedom.

Next, the force constants were fitted to the AM1 data. The force field fit program we developed reads the AM1 calculated heats of formation as well as the atomic coordinates of the molecule. Average (AM1 calculated)

Table V
AM1 Calculated Partial Charges for the Extension Unit of PHNA (for Comments See Text)

atom no.	atom	type	charge	atom no.	atom	type	charge
42	C	65	+0.09	52	H	10	+0.15
43	C	65	−0.14	53	H	10	+0.14
44	C	66	−0.09	54	H	10	+0.16
45	C	65	−0.07	55	H	10	+0.16
46	C	66	−0.04	56	H	10	+0.15
47	C	65	−0.12	57	H	10	+0.15
48	C	65	−0.08	58	C	63	+0.36
49	C	66	−0.13	59	O	85	−0.33
50	C	65	+0.01	60	O	83	−0.23
51	C	66	−0.14				

Table VI
AM1 Calculated Partial Charges for the Extension Unit of PHBA (for Comments See Text)

atom no.	atom	type	charge	atom no.	atom	type	charge
30	C	65	+0.11	37	H	10	+0.16
31	C	65	−0.16	38	H	10	+0.16
32	C	65	−0.05	39	H	10	+0.16
33	C	65	−0.13	40	C	63	+0.36
34	C	65	−0.05	41	O	85	−0.33
35	C	65	−0.16	42	O	83	−0.23
36	H	10	+0.16				

Table VII
Fitted Force Field Parameters for the Valence Angles

type of valence	force field	av angle
65/66–65–63	60	120
65–63–83	80	113
65–63–85	80	129
83–63–85	80	118
63–83–65	180	115
83–65–65/66	90	120
10–80–65	133	108.1
80–65–65	80	120
65–63–80	80	114
85–63–80	80	117
63–80–10	113	109.8

values for the bond lengths were employed (bond lengths were assumed to be constant in the force field (see previous section)). For the fitting of bending and improper torsion force constants, additional AM1 data were used that had been obtained on structures for which these geometrical variables were varied in 1° steps. Although basically clear from the previous section (section 3), we note that both the LJ parameters and the atomic charges were not varied while the force field was fit but given the values discussed in the previous section, whereas all other parameters were adjusted to the AM1 data.

To obtain the correct rotational barriers, we have used the scaling factor that was introduced by Coussens et al.[2] In effect, the resulting torsional energy *differences* of the heats of formation were scaled by the factor 1.9.

The fitting process was carried out iteratively rather than as a one-step process. In more detail, the *E* barrier was fitted first. Subsequently, the barrier *G* was fitted and finally barrier *F*. In the latter process the torsional map *F*–*G* was employed in addition. The fitted data were compared with the original (though scaled, factor 1.9) AM1 data, and if not in sufficient agreement, the fitting was restarted from that point with a refit of the *E* potential energy curve and so on. An additional requirement with respect to the similarity between AM1 and fitted FF data was that the minimum energy geometries should be close.

First, in the actual fitting process the force field for PHNA was fitted in the way just described. The force field parameters obtained have been collected in Table VII (valence angle FF parameters), Table VIII (torsional FF parameters), and Table IX (improper torsion FF

Table VIII
Fitted Torsional Force Field Parameters

torsional angle type	force field parameter (kcal/mol) $H_{1\phi}$	$H_{2\phi}$	$H_{3\phi}$	$H_{4\phi}$	torsion type
65/66–65–63–83	0	0.624	0	0.024	E
65/66–65–63–85	0	0.624	0	0.024	E
65–63–83–65	0	2.51	0	–0.030	F
85–63–83–65	2.79	2.51	0.210	–0.030	F
63–83–65–65	0	1.02	0	–0.170	G
63–83–65–66	0.591	0.672	0.224	–0.165	G[a]
65/66–65–80–10	0	1.50	0	0	
65/66–65–63–80	0	0.642	0	0	
65–63–80–10	0.47	4.48	–0.44	0	
85–63–80–10	3.26	2.18	0.18	0	

[a] These values apply to HNA only.

Table IX
Fitted Force Field Parameters for the Improper Torsions[a]

type of improper torsion	force field parameter $H_{2\phi}$ (kcal/mol)
63–65–65/66–65/66[b]	7.5
65–63–83–85	17.5
65–63–85–83	17.5
85–63–83–65	17.5
85–63–65–83	17.5
83–63–65–85/83–63–85–65	17.5
83–65–65/66–65/66[b]	15
80–65–65/66–65/66[b]	7.5
65–63–80–85	7.5
65–63–85–80	7.5
85–63–65–80	7.5
85–63–65–80	7.5
85–63–80–65	7.5
80–63–65–85	7.5
80–63–85–65	7.5

[a] In the term describing the improper torsion the second atom type (*j* in the sequence *ijkl*) is the central atom. [b] All four combinations to be obtained by mutating the 65 and 66 in the third and fourth positions basically have the same force field parameter, but the 65–66 combination does not appear in practice in our systems.

parameters). Then going over to PHBA, the same Lennard-Jones parameters were used as for PHNA, and the AM1 calculated charges were adopted (differences between AM1 calculated charges between PHNA and PHBA are small and typically less than 0.02 charge unit). The force field parameters corresponding to the valence, torsional, and improper torsional terms in the force field eq 1 were transferred from PHNA to PHBA except for the parameters relating to torsion *G*. The justification of adopting this transferrability will be shown later when the AM1 calculated and the fitted force field potential energy curves are compared (see subsequent section). Coming back to the *G* torsion parameters, an energy difference between the $G = 0°$ and $G = 180°$ conformations occurs for PHNA, a phenomenon which does not occur for PHBA. This effect for PHNA is caused by the nonequivalence of the naphthalene carbon atoms C_{23} and C_{27}, which in turn is caused by electronic effects due to the asymmetric attachment of the second ring in HNA as compared to HBA. In our fitted force field we have reflected this difference by adapting the torsional potentials, i.e., introducing a difference between the torsions C_{19}–O_{21}–C_{22}–C_{23} and C_{19}–O_{21}–C_{22}–C_{27} in PHNA. In PHBA these torsions are equivalent. However, with respect to general applicability of the force field expression, both for PHNA *and* PHBA, both terms are present explicitly as the torsional potentials are given as a sum of the torsional potentials of all relevant atom combinations, i.e., torsions *F* and *G* consist of two contributions (for PHBA the atom sequences are 2–3–4–5 and 19–3–4–5 for the *F* torsion and 3–4–5–6 and 3–4–5–13 for the *G* torsion), whereas for torsion *E* there are four relevant contributions (for PHBA the atom combinations are 1–2–3–4, 1–2–3–19, 17–2–3–4, and 17–2–3–19). Table VIII contains the torsional force field parameters we have thus obtained.

As a final test, the transferrability of the force field parameters was tested on the rotational barrier of the carboxyl group in benzoic acid. The latter is a small species for which we think a reliable rotational barrier for the free molecule is available from the scaled AM1 data of the work of Coussens et al.[2]

5. Results of Force Field Fit Procedure

Figure 1 shows the explicit structures on which the AM1 calculations were carried out, i.e., dimers of PHBA and PHNA and trimers of PHBA and PHNA ($n = 3$), for obtaining information on extension units for PHBA and PHNA (for further explanation see later), and, as announced in the above, benzoic acid. Figures 2–4 show the scaled AM1 as well as the fitted force field calculated torsional potentials *E*, *F*, and *G* in PHBA, respectively. In Figure 5a the two-dimensional map of the potential energy as a function of the dihedrals *F* and *G* in PHBA has been depicted. Figure 5b shows the corresponding force field plot. The corresponding results obtained for PHNA are so similar to those for PHBA that showing all figures for PHNA that correspond to Figures 2–5 for PHBA was considered superfluous.

Comparison of the scaled AM1 calculated data and the fitted force field data displayed in Figures 2–5 clearly illustrates that the force field fit which was predominantly focused on a good representation of the torsional potentials is good. Geometrical data as obtained from force field and AM1 energy minimizations have been collected in Table X for PHBA (the average differences with PHNA are about 1°). The good fit for PHBA illustrates that the parameters are transferrable from PHNA to PHBA. Such a feature is of substantial importance because the absence of such a correspondence would lead to a different force field for each different species, making the approach practically worthless for general use.

As an additional test we employed the force field parameters fitted to PHBA/PHNA to calculate the rotational barrier for the ester group in benzoic acid (cf. the *E* torsion in PHBA and PHNA). The resulting value of 5.51 kcal/mol compares favorably to the value of 5.35 kcal/mol from the scaled AM1 data,[2] a result which once more illustrates the transferrability and accuracy of our newly developed force field parameters. As an alternative one could adopt the parameter values for the terminal free carboxylic groups in PHNA and PHBA and use these for benzoic acid. This leads to a force field calculated barrier of 5.63 kcal/mol. The agreement among these three values is very satisfactory indeed as compared to the current state of calculated values for rotational barriers in these conjugated polymeric systems (for a short review see ref 1a).

When we want to model long polymeric chains, it is required to have a force field available for a monomer extension unit, as explained previously. With respect to a monomer extension unit, we have already indicated that electroneutrality is required to have an electrically neutral polymer chain as discussed before. It turned out directly from the calculated AM1 results that the overall charge on the central monomer of the trimers was already practically neutral. The charges thus obtained are in very good agreement with those obtained on the dimer (compare Tables IV and VI for PHBA and Tables III and V for PHNA).

To demonstrate that we have obtained a *proper* force field for modeling the conformational properties of some

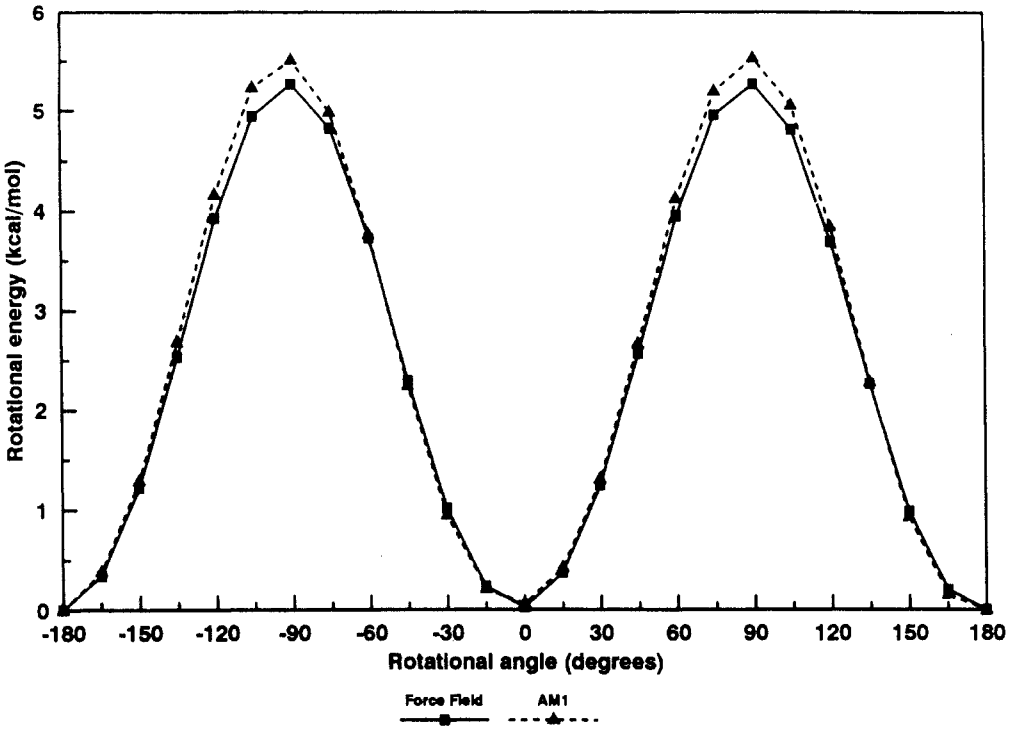

Figure 2. Torsional energy for torsion E of PHBA calculated according to the AM1 method (including scale factor of 1.9) and the newly derived force field.

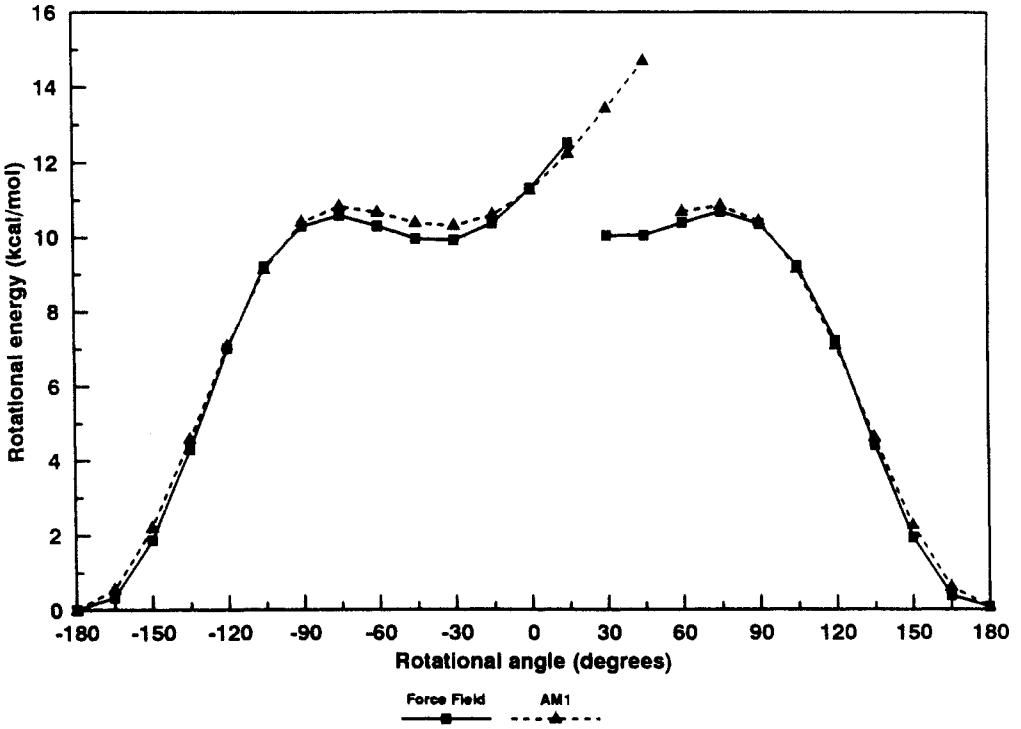

Figure 3. Torsional energy for torsion F of PHBA calculated according to the AM1 method (including scale factor of 1.9) and the newly derived force field. The fact that the curve is interrupted is the result of displaying the actual results of the calculations, in which concerted motion causes the structure to move to another local minimum energy structure than looked for. For further explanation see section 4.

aromatic polyesters, Table XI contains some bond angle and valence (bond) angle values as corroborated from the new force field, from the AM1 calculations, and from experimental data as retrieved from the Cambridge Crystallographic Data Bank and tabulated by Coulter and Windle.[13] The experimental data quoted are the "idealized" values from Coulter and Windle's table, i.e., those for "essentially the mean geometry after excluding unexpectedly deviant values from the calculation".[13] In the parameters of the new force field the bond angles were kept fixed at their AM1 calculated values (see previous sections), and thus only one set (AM1/new FF) of values is presented in Table XI. The values as corroborated from the new force field agree well with the AM1 results, as well as with the experimental data: typical differences are 0.02 Å for bond lengths and 0–3° for valence angles. As expected, the packing of the molecules (the experimental data evidently correspond to bulk material) does not affect bond length and bond angles to any significant extent.

As far as torsional angles are concerned, a direct comparison with experimental data as obtained from crystallographic data is not appropriate, for the intermolecular forces between the polymer chains will affect the torsional angles so as to result in proper packing of the

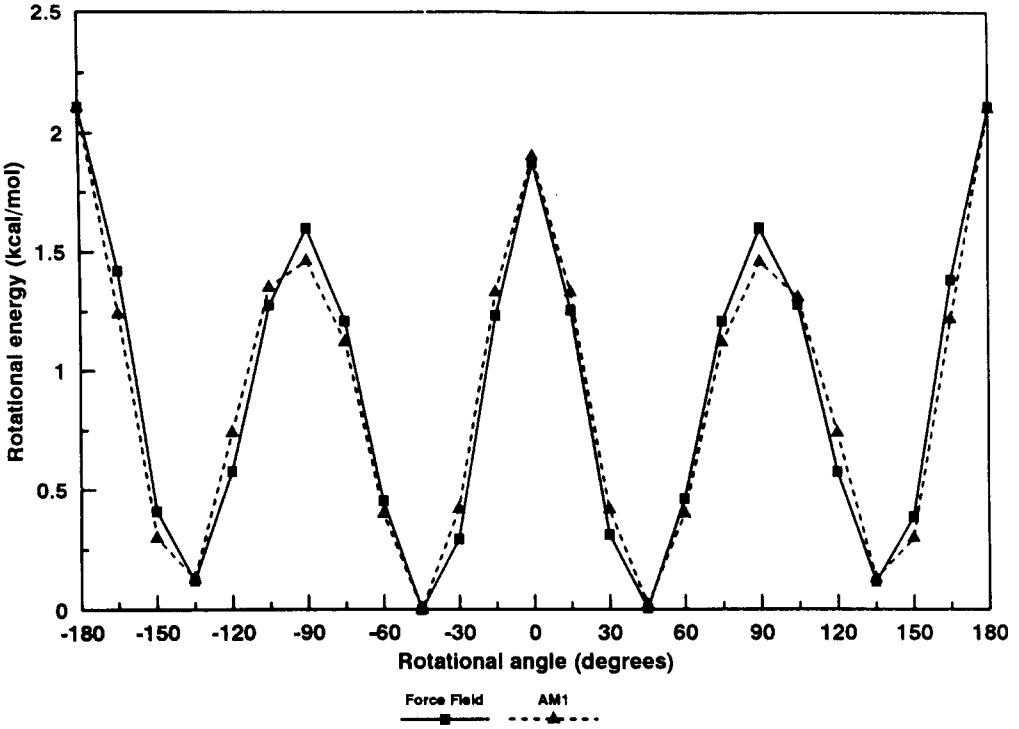

Figure 4. Torsional energy for torsion G of PHBA calculated according to the AM1 method (including scale factor of 1.9) and the newly derived force field.

chains in the crystal. However, we believe we have well-calibrated our torsional barriers by the procedure outlined in ref 2 and based on a careful study of similar rotations in small aromatic moieties. The procedure turned out to be accurate within about 15%, a result which has not yet been surpassed by any other method.

On the basis of these results we think we have obtained a qualified force field for modeling the single-chain conformational characteristics of the aromatic polyesters PHBA and PHNA and their copolymers. The accuracy of the geometrical parameters, as corroborated from the comparison presented in the above, seems necessary, but perhaps not even sufficient, when conformational properties such as the characteristic ratio are calculated. In a recent paper Mattice[14] has demonstrated that torsional angle deviations of typically 5° may lead to a 10% variation in the calculated characteristic ratio (for details see Mattice[14]).

Finally we want to comment on the applicability of the new force field obtained in vacuo for "real" polymer chains. Formally, the present parametrization is perhaps considered appropriate for gas-phase molecules void of intermolecular interaction only, for we have calibrated the rotational barriers to experimental gas-phase data intending to develop a force field with an appropriate separation between intra- and intermolecular interactions. With only the intramolecular interactions taken into account, we effectively have a "polymer chain in vacuo" potential. This is what we have accomplished in the first place, i.e., employed semiempirical calculations on free molecules, added to that the calibration of the rotational barriers based on free molecule experimental data. The next question then is, to what extent does our potential account for intermolecular interactions? The intermolecular interactions in the force field expression eq 1 are the van der Waals and the Coulombic terms only. The van der Waals term, i.e., modeled by a Lennard-Jones potential, was taken from the AMBER force field. It remains to be tested in real simulations on bulklike systems whether the Lennard-Jones parameters used are the best ones for the aromatic polyesters, but due to its success in other fields of application, the present set is expected to be not too far off. Next, the charges were taken from the AM1 calculations. The charges on the atoms hardly change when one goes from a single chain to bulk. On one hand we have checked this by energy-minimizing a cluster of PHBA dimers, and on the other hand it is a known fact from XPS spectroscopy on polymers that the difference between gas-phase and solid-state inner shell ionization energies (the latter being determined by the atom's charge) is solely due to differences in work function. Consequently, the charges need not be adapted to the bulk situation, but the correctness of the charges nevertheless remains a matter of concern.

So finally we conclude that, on the basis of the discussion above, the force field developed is appropriate for gas-phase molecules and also for real polymers, i.e., bulk material, with the annotation that the absolute values of the charges as well as the precise values of the Lennard-Jones parameters need further inspection. The latter is a problem also often overlooked and to our understanding not well-covered in many force field parametrizations. It can only be effectuated after simulations on bulk polymer are carried out and the results of such simulations are compared with the appropriate experimental data. Such a comparison has not yet been carried out by us so far.

6. Molecular Dynamics Simulations on PHNA and PHBA

In the first paper of this series one section (section 4d) was devoted to molecular dynamics (MD) simulations. Some results were presented on simulations of polyethylene, poly(ethylene terephthalate), poly(*p*-hydroxybenzoic acid), and polyphenyl. These simulations were definitely not aimed at being of good quality with respect to requirements one ought to impose for obtaining realistic values for quantities such as the persistence length. They demonstrated the fact that the conformational behavior of the polymer chains critically depends on the quality of the intra- and interchain potentials. In the present paper we have developed proper *intra*molecular potentials for PHNA and PHBA. Subsequently, to illustrate the fact

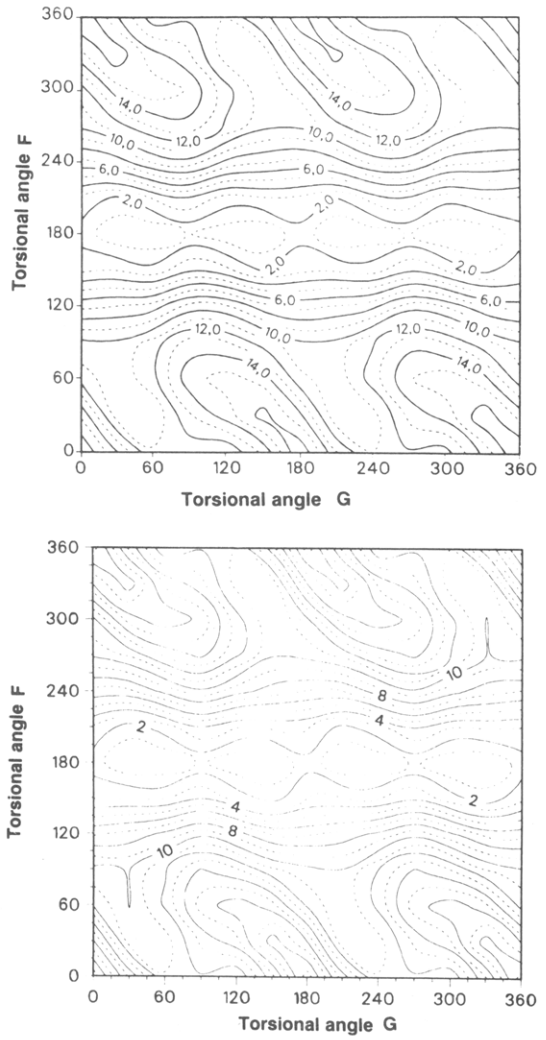

Figure 5. Two-dimensional map displaying the potential energy as a function of rotation around torsional angles F and G in PHBA as obtained from (a, top) calculations involving the AM1 method (including scale factor of 1.9) and (b, bottom) calculations with the newly derived force field. The values in the plot are relative energies in kilocalories per mole. Note that there is an additional variation of the angle E that could not be displayed simultaneously.

that our new force field yields averages and root mean square deviations of geometrical parameters that are (substantially) different from those based on a "standard" force field (see ref 1a), MD simulations were carried out at 600 K and over a time span of 100 ps with 2-fs time steps on a 30-monomer chain of PHBA. In the MD simulations structures were stored every 5 ps. The MD results employing the CV force field (cf. ref 1a) are to be compared to those obtained with the new force field derived here.

Referring to the discussion in refs 1b,c, again we do not suggest that these simulations allow for abstracting realistic values for properties such as the persistence length of the polymer chain. We are aware of the fact that these simulations are indeed vacuum simulations and that the results are not intended to say anything on bulk properties. Here we only pursue to show the differences when employing the new force field.

To demonstrate the changes in flexibility of the polymer chain when employing our newly derived force field as compared to the CV force field, we have compared the average and rms valence and torsional angles of the ester linkage in PHBA as obtained from MD simulations employing the CV force field, which has too high rotational barriers, and our improved force field. In the case of

Table X
Comparison of Geometries for PHBA As Obtained from AM1 Data and from Fitted Force Field (Geometry Referred to in the Last Part of This Table Corresponds to the Data Point $F = 0°$, $G = 90°$)

	torsional angle (deg)			valence angle (deg)				
	E	F	G	1–2–3	19–3–4	2–3–4	3–4–5	4–5–6
Rotation around Torsion G								
FF	3	174	180	122.5	123.9	111.5	123.9	112.1
AM1	6	171		121.9	120.1	112.1	124.3	112.0
FF	1	179	135	122.3	121.0	112.7	119.5	116.7
AM1	3	180		121.7	118.6	112.9	119.8	115.7
FF	3	179	90	122.1	118.5	113.9	116.3	119.2
AM1	0	180		121.7	118.1	113.2	118.5	119.3
FF	5	175	45	122.3	120.9	112.9	119.3	121.8
AM1	4	179		121.7	118.7	112.9	120.2	123.2
FF	3	174	0	122.5	123.9	111.5	123.8	126.6
AM1	4	178		121.9	120.2	112.1	124.4	127.2
Rotational Barrier E								
FF	90	177	42	119.8	122.2	111.1	119.5	117.5
AM1		180	38	119.8	120.7	111.5	120.7	115.1
1								
Conformation at the Point $F = 0°$, $G = 90°$								
FF	86	0	90	119.3	116.8	116.3	117.8	119.5
AM1	70			118.4	110.6	119.5	119.5	119.1

Table XI
Comparison of Geometrical Parameters As Obtained from the New Force Field on PHBA, AM1 Data on PHBA, and Experimental Geometrical Parameters of Aromatic Polyesters Containing the Phenyl Benzoate Moiety[13] (Numbering Refers to PHBA Dimer Depicted in Figure 1)

bond length (Å)	AM1/new FF	exptl[13]
2–3	1.47	1.48
3–19	1.23	1.20
3–4	1.38	1.36
4–5	1.39	1.41

valence angle (deg)	AM1	new FF	exptl[13]
1–2–3	122.3	121.8	122.5
2–3–4	112.3	112.6	111.7
3–4–5	121.5	121.5	118.8

Table XII
Mean Values and Root Mean Square Fluctuations of Valence and Torsional Angles in PHBA When the Consistent Valence Force Field (CVFF) and Our New Force Field (New FF), Respectively, Were Employed

type of valence/dihedral angle in PHBA	mean angle (deg), CVFF/new FF	rms fluctuation (deg), CVFF/new FF
C_2–C_3–O_4	118.0/113.2	3.0/4.9
C_3–O_4–C_5	120.0/118.3	4.5/4.1
E (C_1–C_2–C_3–O_4)		15/35
F (C_2–C_3–O_4–C_5)		30/17
G (C_3–O_4–C_5–C_6)	comparison not useful; for explanation see text	

multiple minima, the rms deviations were calculated by relating all angle values to one particular valley (i.e., by shifting the angle values to the corresponding value within that single-valley range). The values obtained by employing the CV force field as well as those obtained from the fitted force field have been collected in Table XII. We observe a 5° decrease in the valence angle C_2–C_3–O_4 when comparing the CV force field and the fitted force field averaged values. The fitted force field value is very close to the original AM1 result for this entity. More importantly, the AM1 value for this angle is close to the value of 112° given by Coulter and Windle[13] as the average over a series of crystal structures of molecules containing the phenyl benzoate moiety. The average of the adjacent C_3–O_4–C_5 bond angle is slightly decreased by 2° when going from the CV force field to the new force field. An

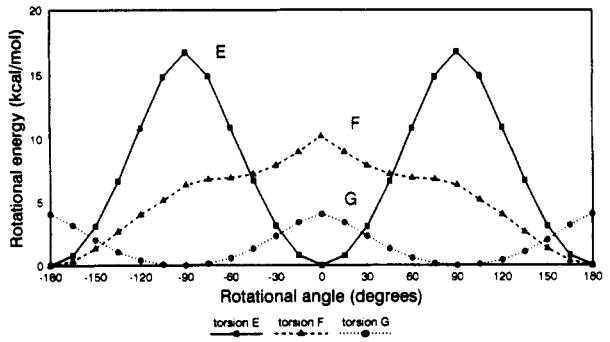

Figure 6. CVFF-calculated rotational energy profiles for torsional angles E–G in PHBA. The marks on the curves indicate the data points that were calculated explicitly.

interesting chain property such as the persistence length is intimately related to chain flexibility; the latter property is determined both by the collinearity and the rotatability of the chain constituents. Important factors determining the collinearity are the rms deviation of the F torsion and the values of the valence angles C_2–C_3–O_4 and C_3–O_4–C_5 just discussed. The deviation from collinearity between the bonds C_2–C_3 and C_4–C_5 in the ester linkage at F = 180° increased from 2° in the CV force field to 5° in the new force field (on the basis of data given in Table XII).

As far as the rms torsional deviations are concerned, the deviations in the E torsional angle were substantially larger in the fitted force field simulation than in the CVFF MD simulation, thus increasing the rotatability. This is qualitatively fully understandable when the corresponding potential energy curves, i.e., Figures 2 and 6, respectively, are compared. For torsion F, however, the rms deviation obtained from the MD results using the fitted force field is substantially *smaller* than those obtained on the basis of the CV force field, which reduces the deviation from collinearity: the chains are stiffer. This can also be understood semiquantitatively when the fitted force field (i.e., scaled AM1) barriers are compared with those from the CVFF, i.e., compare Figures 3 and 6 for torsion F. Here it is not the barrier heights that account for the difference but the steepness of the barrier as seen from the minimum energy structure. Finally, with respect to torsion G, a comparison between rms torsional fluctuations from the MD simulations is not useful because of the *qualitative* differences in the torsional energy profiles (cf. Figures 4 and 6): the CVFF yields two minima, whereas the newly derived force field (and so the AM1 data) yields four. The shallowness of the CVFF rotational energy curve for the G torsion (Figure 6) as compared to the result obtained on the new force field, whereby we also consider the absolute barrier heights, indicates that the actual rotatability is larger for the CVFF case than with the new force field. As expected, almost identical results were obtained for PHNA, for the torsional potentials are very much alike.

In conclusion, we have only discussed the differences in rms deviations qualitatively. When trying to make a more quantitative statement on the comparison between the rms deviations as corroborated from the MD simulations and the potential energy curves as obtained from the CV force field and the fitted force field, respectively, it should be borne in mind that appreciable concerted motion between the torsional motions occurs (see ref 1a). The increased rotatability around torsion E and the decreased rotatability around torsion F, as corroborated from the new force field results as compared to the CV force field and collected in Table XII, do not unambiguously tell us whether the overall flexibility of the chain has either increased or decreased on going from the CV force field to the new force field. The reason is that Table XII contains rms fluctuations, but any actual correlations due to concerted motion are not explicit. Concerted motions might co-add or counteract each other, thereby either increasing or decreasing overall flexibility, respectively. It is only from decent simulations (to be carried out) and their proper analysis that such conclusions might be drawn. However, the differences between the results of the MD simulations employing the CV force field and those employing the newly derived force field, respectively, do show appreciable differences (cf. Table XII) and as such justify the development of the new especially designed force field.

Acknowledgment. We thank the referees for their useful criticism of the first version of this paper. We gratefully acknowledge the management of DSM Research for their permission to publish this work. We also acknowledge M. Schlenkrich and K. Nicklas of TH Darmstadt for making available the MD program and for help with running it, respectively.

References and Notes

(1) (a) Lautenschläger, P.; Brickmann, J.; van Ruiten, J.; Meier, R. J. *Macromolecules* **1991**, *24*, 1284. (b) Jung, B.; Schürmann, B. *Macromolecules* **1992**, *25*, 1003. (c) Lautenschläger, P.; Brickmann, J.; van Ruiten, J.; Meier, R. J. *Macromolecules* **1992**, *25*, 1004.
(2) Coussens, B.; Pierloot, K.; Meier, R. J. *J. Mol. Struct. THEOCHEM.* **1992**, *259*, 331.
(3) Dewar, M. J. S.; Zoebisch, E. G.; Healy, E. F.; Stewart, J. J. P. *J. Am. Chem. Soc.* **1985**, *107*, 3902.
(4) Stewart, J. J. P. *J. Comput. Chem.* **1989**, *10*, 209.
(5) Stewart, J. J. P. *J. Comput. Chem.* **1989**, *10*, 221.
(6) Program 455 from Quantum Chemistry Program Exchange, Creative Arts Building 181, Indiana University, Bloomington, IN 47405.
(7) For a partial description of this force field see: Hagler, A. T. *J. Am. Chem. Soc.* **1979**, *101*, 5122.
(8) Models using software programs from BIOSYM Technologies of San Diego—computed with DISCOVER and displayed using Insight II.
(9) Ryckaert, J. P.; Ciccotti, G.; Berendsen, H. J. C. *J. Comput. Chem.* **1977**, *23*, 327.
(10) Ciccotti, G.; Ferrario, M.; Ryckaert, J. P. *Mol. Phys.* **1982**, *47*, 1253.
(11) Weiner, S. J.; Kollman, P. A.; Nguyen, D. A.; Case, D. A. *J. Comput. Chem.* **1986**, *7*, 230.
(12) Henderson, D. *Annu. Rev. Phys. Chem.* **1974**, *25*, 461.
(13) Coulter, P.; Windle, A. H. *Macromolecules* **1989**, *22*, 1129.
(14) Mattice, W. L. *Comput. Polym. Sci.* **1991**, *1*, 173.